J. Phys. B: At. Mol. Opt. Phys. **40** (2007) 943–954 doi:10.1088/0953-4075/40/5/010

Many-electron model for multiple ionization in atomic collisions

C D Archubi[1], **C C Montanari**[1,2] **and J E Miraglia**[1,2]

[1] Instituto de Astronomía y Física del Espacio, Casilla de Correo 67, Sucursal 28, (C1428EGA) Buenos Aires, Argentina
[2] Departamento de Física, Facultad de Ciencias Exactas y Naturales, Universidad de Buenos Aires, Buenos Aires, Argentina

E-mail: archubi@iafe.uba.ar

Received 8 November 2006, in final form 3 January 2007
Published 19 February 2007
Online at stacks.iop.org/JPhysB/40/943

Abstract
We have developed a many-electron model for multiple ionization of heavy atoms bombarded by bare ions. It is based on the transport equation for an ion in an inhomogeneous electronic density. Ionization probabilities are obtained by employing the shell-to-shell local plasma approximation with the Levine and Louie dielectric function to take into account the binding energy of each shell. Post-collisional contributions due to Auger-like processes are taken into account by employing recent photoemission data. Results for single-to-quadruple ionization of Ne, Ar, Kr and Xe by protons are presented showing a very good agreement with experimental data.

1. Introduction

Multiple ionization is still a complex problem in atomic collisions. Theoretical models, based on distorted wave methods [1, 2] or time-dependent solutions of the Schrödinger equation [3, 4], describe reasonably well the experimental values for single-ionization cross sections. Difficulties increase in the cases of multiple ionization because there are many processes to be considered (direct multiple ionization of outer-shells, inner-shell ionization followed by relaxation processes or accompanied by Auger-like emission). It has been only recently that the combination of the independent particle model (IPM) and the ratios of multi-charged ion production in photoionization experiments has led to satisfactory results for multiple ionization in the MeV regime, where Auger-like processes play a relevant role [5, 6].

Almost all theoretical efforts in the calculation of multiple ionization cross sections are based on variants of the IPM [5–8], followed by a multinomial statistics. The aim of this work is to present an alternative approach based on a many-electron description to deal with complex systems. The collective representation of the electron cloud led to a simple formalism

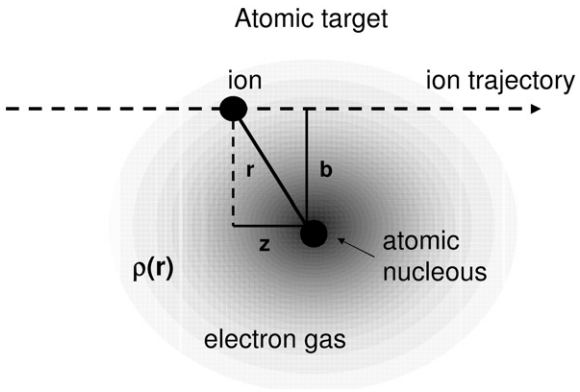

Figure 1. Scheme of the collision between the ion and the target electrons.

which do not require high computing power, and let us describe Ne or Xe targets with the same degree of complexity.

This approach lies upon three theoretical developments. (i) We solved the transport equation [9–15] for an ion travelling through a single atom (inhomogeneous electronic density), leading to the Poisson distribution, instead of the multinomial one. (ii) We improved the shellwise local plasma approximation (SLPA) [16, 17] to obtain the single-ionization probabilities as a function of the impact parameter. The present version employs the Levine and Louie dielectric function [18], instead of the one by Lindhard [19], to take into account the energy ionization threshold of each shell. (iii) We included the post-collisional contributions (time delay vacancy production following direct ionization of inner shells) in the Poisson distribution by employing ratios of charge state distribution of the target atoms measured with time-of-flight (TOF) spectroscopy and photoelectron-ion coincidence techniques [20–31] .

The work is organized as follows. In section 2, we present the three theoretical developments mentioned above. In section 3, the results for single, double, triple and quadruple ionization of rare gases (Ne, Ar, Kr and Xe) by protons are displayed and compared with the experimental data. Finally, the conclusions are presented in section 4. Atomic units are employed throughout this work, except when it is especially mentioned.

2. Theoretical model

2.1. The transport equation for ion-electron scattering inside the atom

We consider an incident ion beam with energy E_0 moving in the direction z into an atom with many electrons. The electrons are represented by their density $\rho(r)$, with $\boldsymbol{r} = \boldsymbol{z} + \boldsymbol{b}$ being the position with respect to the target nucleus, and with b being the impact parameter (see figure 1). Assuming that the change in the electronic distribution is negligible after each collision (many-electron approximation) and using the linearized Boltzman equation for the interaction of the ion with the electron cloud, the transport equation for the projectile energy distribution $g(E, z, b)$ is given by

$$\frac{\partial g(E,z,b)}{\partial z} = \int_0^{E_0} \mathrm{d}\omega W(\omega, z, b)[g(E+\omega, z, b) - g(E, z, b)]. \tag{1}$$

This is the Landau equation for multiple scattering, where the kernel $W(\omega, z, b)$ is the collision probability per unit path length and per energy transfer ω to the target electrons. The limits of

the ω integration in (1) are due to the energy conservation, where E_0 is the maximum energy the projectile can transfer. These limits can be extended to the whole energy range changing $W(\omega, z, b)$ by $W(\omega, z, b)\Theta(\omega)\Theta(E_0 - \omega)$.

By following the usual procedure to solve the transport equation [13], we change to the Fourier space, and express $g(E, z, b)$ as

$$g(E, z, b) = \int_{-\infty}^{+\infty} \frac{\mathrm{d}t}{2\pi} \exp[\mathrm{i}(E_0 - E)t]\widetilde{g}(t, z, b), \tag{2}$$

where the tilde represents the Fourier transform. We find the solution

$$\widetilde{g}(t, z, b) = \exp[Q(t, z, b) - Q(0, z, b)],$$

with

$$Q(t, z, b) = \int_{-\infty}^{z} \mathrm{d}z' \widetilde{W}(t, z', b), \tag{3}$$

and

$$\widetilde{W}(t, z, b) = \int_{-\infty}^{+\infty} \mathrm{d}\omega \exp[-\mathrm{i}\omega t] W(\omega, z, b). \tag{4}$$

For a constant electronic density (i.e. free conduction electrons of a metal foil), $\widetilde{W}(t, z, b)$ becomes independent of z and b. In this case, integrating (3) from 0 to z gives $Q(0, z, b) = z\widetilde{W}(0, 0, 0) = z\int_{-\infty}^{+\infty} \mathrm{d}\omega W(\omega, 0, 0)$, which is the result of Lencinas and Burgdörfer [13].

If we expand the exponential function $\exp[Q(t, z, b)]$ into a power series, we can express $g(E, z, b)$ as

$$g(E, z, b) = \sum_{N=0}^{\infty} g_N(E, z, b), \tag{5}$$

with

$$g_N(E, z, b) = \exp[-Q(0, z, b)] \int_{-\infty}^{+\infty} \frac{\mathrm{d}t}{2\pi} \exp[\mathrm{i}(E_0 - E)t] \frac{[Q(t, z, b)]^N}{N!}. \tag{6}$$

Integrating $g_N(E, z, b)$ over all the possible energies we obtain

$$G_N(z, b) = \int_{-\infty}^{+\infty} \mathrm{d}E g_N(E, z, b), \tag{7}$$

$$= \exp[-Q(0, z, b)] \frac{[Q(0, z, b)]^N}{N!}, \tag{8}$$

which is the well-known Poisson distribution. The function $G_N(z, b)$ is expressed in terms of a multiple scattering expansion, where N can be understood as the number of inelastic collisions of the projectile with the electrons in the atom [13]. As expected, $G_N(z, b)$ given by (8) verifies the unitarity condition $\sum_{N=0}^{\infty} G_N(z, b) = 1$.

As we are dealing with atomic collisions, we are interested in the probabilities of inelastic transitions considering the integration in z from $-\infty$ to ∞, that is $p(b) = Q(0, \infty, b)$. This probability relates to the kernel of (1) as

$$p(b) = \int_{-\infty}^{\infty} \mathrm{d}z \int_{-\infty}^{\infty} \mathrm{d}\omega W(\omega, z, b). \tag{9}$$

Note that $p(b)$ is the probability per atom. It takes into account all the target electrons, and may be larger than unity, meaning that more than one electron is ionized. Instead, the probabilities per electron (single-collisional event, IPM) must be rigorously smaller than unity.

The Nth term of the Poisson distribution $G_N(\infty, b) = P_N(b)$ gives the probability of excitation of N electrons

$$P_N(b) = \frac{[p(b)]^N}{N!} \exp[-p(b)], \tag{10}$$

with the term $N = 0$, being the elastic case $P_0(b) = \exp[-p(b)]$ and $\sum_{N=0}^{\infty} P_N(b) = 1$. The N excitation cross section is given by

$$\sigma_N = 2\pi \int_0^{\infty} P_N(b) b \, \mathrm{d}b, \tag{11}$$

and the total inelastic cross section, $\sigma = 2\pi \int_0^{\infty} p(b) b \, \mathrm{d}b$, satisfies $\sigma = \sum_{N=1}^{\infty} N\sigma_N$.

2.2. The SLPA applied to ionization

The kernel $W(\omega, z, b)$ of the transport equation (1) represents the collision probability per unit path length. To obtain this, we resort to the SLPA [16, 17], which is a many-body formulation based on the dielectric formalism to deal with the interaction of the ion with the electron cloud. It is a known model supported by three basic assumptions:

(1) $W(\omega, z, b)$ is derived from the dielectric formalism [32, 33];
(2) the bound electrons can be described as an inhomogeneous free electron gas of local density $\rho_{\mathrm{nl}}(r)$ and Fermi velocity $k_{\mathrm{nl}}^F(r) = [3\pi^2 \rho_{\mathrm{nl}}(r)]^{1/3}$;
(3) the response of these electrons to the ion perturbation can be considered shell-to-shell (independent-shell approximation) with their corresponding binding energies.

Besides these hypothesis, the SLPA is a first-order approximation for a projectile moving in a free electron gas, so it is valid in the perturbative region, i.e. $Z_P/v < Z_T$ and $v > k_{\mathrm{nl}}^F(r)$.

In the SLPA, each electron is a part of a whole (the electrons of the same shell), screening the impinging ion along its path. The seminal developments on the local plasma approximation (LPA) were made during the 1960s and 1970s [34–37]. However, the present SLPA introduces modifications on the original formalism based on the shell-to-shell treatment [16, 17, 38], and it has already been employed in the calculation of total ionization cross sections of gas and solid targets [16, 39–42] with good results.

Consider a bare ion of charge Z_P moving with a velocity v in a free electron gas of inhomogeneus density $\rho(r)$. The target nl shell is characterized by its electron density $\rho_{\mathrm{nl}}(r) = |\varphi_{\mathrm{nl}}(r)|^2$, with $\varphi_{\mathrm{nl}}(r)$ being the Hartree–Fock wavefunction for neutral atoms [43]. The SLPA probability of inelastic (ionization) transition of the nl shell as a function of the impact parameter b can be expressed as

$$p_{\mathrm{nl}}(b) = \int_{-\infty}^{\infty} \mathrm{d}z \int_0^{\infty} \mathrm{d}\omega \left\{ \frac{2Z_P^2}{\pi v^2} \int_{\omega/v}^{\infty} \frac{\mathrm{d}k}{k} \operatorname{Im}\left[\frac{-1}{\varepsilon(k, \omega, \rho_{\mathrm{nl}}(r))} \right] \right\}, \tag{12}$$

where $\varepsilon(k, \omega, \rho_{\mathrm{nl}}(r))$ is the dielectric function of the nl shell at $r = \sqrt{z^2 + b^2}$. Expression (12) largely differs from the original LPA approximation introduced by Lindhard [34]. Here we follow Levine and Louie [18] to consider the shell energy threshold (binding energy ϵ_{nl} of the state $\varphi_{\mathrm{nl}}(r)$) through the shifted energy transferred. The Levine and Louie $\varepsilon^{\mathrm{LL}}$ dielectric response function is defined as

$$\operatorname{Im}\left[\varepsilon^{\mathrm{LL}}\left(q, \omega, k_{\mathrm{nl}}^F(r)\right)\right] = \begin{cases} \operatorname{Im}\left[\varepsilon^{\mathrm{L}}\left(q, \omega_g, k_{\mathrm{nl}}^F(r)\right)\right] & \omega > |\epsilon_{\mathrm{nl}}| \\ 0 & \omega < |\epsilon_{\mathrm{nl}}|, \end{cases} \tag{13}$$

with $\omega_g = \sqrt[2]{\omega^2 + \epsilon_{\mathrm{nl}}^2}$ and $\varepsilon^L\left(q, \omega, k_{\mathrm{nl}}^F(r)\right)$ being the usual Lindhard dielectric function [19]. This model for the dielectric function, proposed originally for semiconductors and insulators,

satisfies the so-called f-sum rules (particle number conservation), that is a desirable feature for a dielectric function. Note that if we consider no binding energy, $\epsilon_{\rm nl} = 0$, the usual expression for the probability in the dielectric formalism (Lindhard) is recovered. This modified version of the SLPA has also been applied successfully to the calculation of stopping power in insulators [44].

The total ionization probability is obtained as the addition of the shell-to-shell contributions,

$$p(b) = \sum_{\rm nl} p_{\rm nl}(b). \tag{14}$$

The kernel $W(\omega, z, b)$ in (1) is then obtained as

$$W(\omega, z, b) = \sum_{\rm nl} \frac{2Z_P^2}{\pi v^2} \int_{\omega/v}^{\infty} \frac{{\rm d}k}{k} \,{\rm Im}\left[\frac{-1}{\varepsilon^{\rm LL}(k, \omega, \rho_{\rm nl}(r))}\right]. \tag{15}$$

Probabilities and cross sections of N-electron ionization are obtained by introducing the results of (14) in (10) and (11). The total task is a four-dimensional integral on k, ω, z and b.

2.3. The post-collisional contribution

When an inner-shell vacancy is created in an atom, a highly excited state is produced that decays by either radiative transition or electron emission [45]. The post-collisional electron emission, like Auger or Coster–Kroning processes, may be single or give rise to cascades that enhance the number of electrons emitted, i.e. deep vacancies created in direct ionization turn into highly charged ions [20]. Direct ionization takes place in about 10^{-18} s, while the vacancy cascades in the order of 10^{-15} s, and the time of collecting and analysing the ions is about 10^{-5} s, so multiple ionization data correspond to the final ionization states due to the atomic readjustments to inner-shell vacancies [45].

There are several experimental works on multiple emission cross sections of rare gases [5, 8, 46–57] that cannot be explained without including post-collisional contributions in the high energy region, where the inner-shell ionization takes place. The experimental data for double, triple or quadruple ionization cross sections show almost the same slope as the single one [5]. This fact reveals the importance of single ionization followed by Auger emission in multiple ionization at high energies.

The post-collisional processes are approximately independent of the nature of the primary ionization event [46] and can be considered separately. In recent works [5, 6, 57], Auger-like contributions were successfully included in the multiple ionization probabilities of Ne and Ar, as a rearrangement of the multinomial expansion by employing decay rates from photoionization experiments [45].

Formation of multiple-charged rare gas ions in photoionization experiments has been studied by a number of research groups in the latest 15 years by using synchrotron radiation as well as TOF spectroscopy [20–31]. These studies provide fruitful information about yield ratios of multi-charged ions in photoionization experiments. This ratios $F_{{\rm nl},i}$ express how the direct single ionization of a certain nl shell contributes to ion formation of charge $+i$, so that $\sum_i F_{{\rm nl},i} = 1$. Including these ratios in (14) we obtain

$$p(b) = \sum_{\rm nl} p_{\rm nl}(b) \times 1 = \sum_{\rm nl} p_{\rm nl}(b) \times \sum_i F_{{\rm nl},i} = \sum_{i=1}^{Z_T} \mathcal{P}_i(b), \tag{16}$$

with

$$\mathcal{P}_i(b) = \sum_{\rm nl} p_{\rm nl}(b) F_{{\rm nl},i} \tag{17}$$

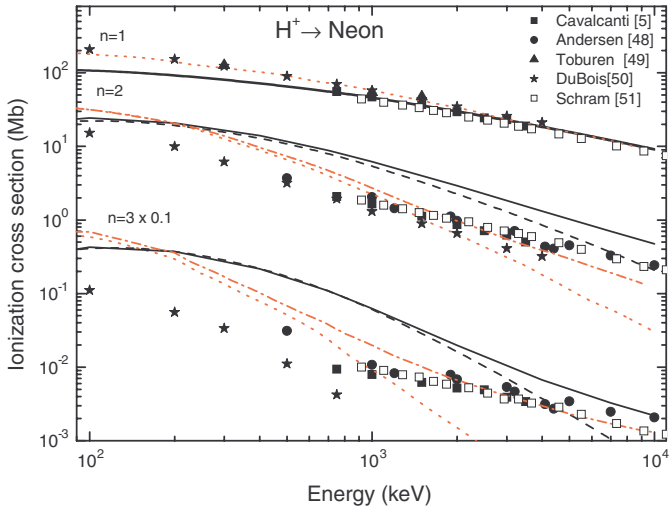

Figure 2. Single ($n = 1$), double ($n = 2$) and triple ($n = 3$) ionization cross sections of Neon by proton impact. Curves: SLPA results with (——) and without (- - - -) post-collisional effects; Kirchner [6] basis generator method with (-.-.-.-) and without (· · · · · ·) post-collisional effects. Experimental data: full symbols, proton impinging data by Cavalcanti *et al* [5], Andersen *et al* [48], Toburen *et al* [49], and DuBois *et al* [50]; open symbols, electron impinging data by Schram *et al* [51].

being the probability of a direct single ionization (of any shell nl) followed by post-collisional emission of $i - 1$ electrons. Replacing (16) in (10) and rearranging terms so as to put together those that contribute to the same number of final emitted electrons, we can express ionization probabilities including post-collisional emission as $P_N^{\rm post}(b)$

$$P_1^{\rm post} = {\rm e}^{-p(b)}\mathcal{P}_1, \tag{18a}$$

$$P_2^{\rm post} = {\rm e}^{-p(b)}\left[\mathcal{P}_2 + \frac{\mathcal{P}_1^2}{2!}\right], \tag{18b}$$

$$P_3^{\rm post} = {\rm e}^{-p(b)}\left[\mathcal{P}_3 + \frac{2\mathcal{P}_1\mathcal{P}_2}{2!} + \frac{\mathcal{P}_1^3}{3!}\right], \tag{18c}$$

$$P_4^{\rm post} = {\rm e}^{-p(b)}\left[\mathcal{P}_4 + \frac{2\mathcal{P}_1\mathcal{P}_3}{2!} + \frac{\mathcal{P}_2^2}{2!} + \frac{3\mathcal{P}_1^2\mathcal{P}_2}{3!} + \frac{\mathcal{P}_1^4}{4!}\right], \tag{18d}$$

where we have shortened $\mathcal{P}_N(b)$ and $P_N^{\rm post}(b)$ by $\mathcal{P}_N$ and $P_N^{\rm post}$. Each expression $P_N^{\rm post}$ includes the term ${\rm e}^{-p(b)}\mathcal{P}_1^N/N!$ that considers all the combination of direct ionization probabilities of N electrons of different shells, and the term ${\rm e}^{-p(b)}\mathcal{P}_N$ that corresponds to a single ionization followed by the emission of $N - 1$ electrons via Auger decay. Other terms combine direct ionization and post-collisional emission so that the ith term is the contribution of the direct ionization of i electrons to final ionization of N ($N - i$ Auger electrons).

3. Results and discussion

We calculate multiple ionization cross sections (single to quadruple) of Ne, Ar, Kr and Xe by protons in the high energy range (0.1–10 MeV). In figures 2 to 5 we display our results

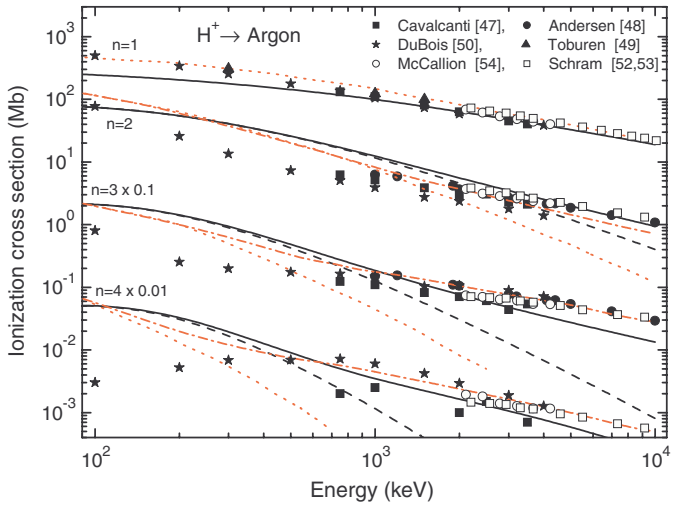

Figure 3. Single ($n = 1$), double ($n = 2$), triple ($n = 3$) and quadruple ($n = 4$) ionization cross sections of Argon by proton impact. Curves as in figure 2. Experimental data: full symbols, proton impinging data by Cavalcanti *et al* [47], Andersen *et al* [48], Toburen *et al* [49], and DuBois *et al* [50]; open symbols, electron impinging data by Schram *et al* [52, 53], and McCallion *et al* [54].

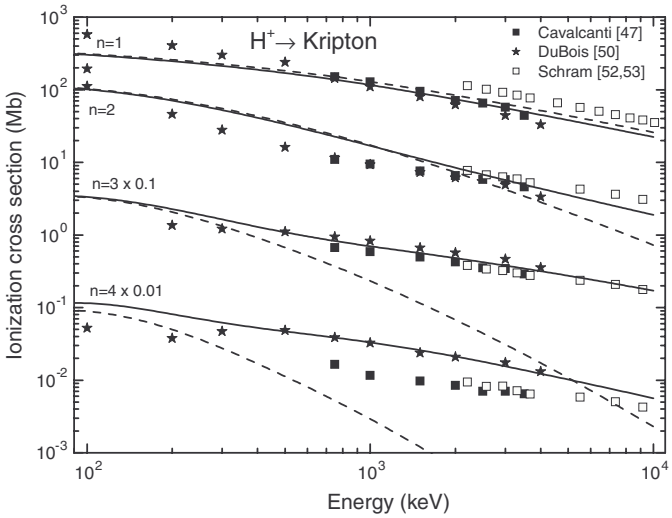

Figure 4. Single ($n = 1$), double ($n = 2$), triple ($n = 3$) and quadruple ($n = 4$) ionization cross sections of Krypton by proton impact. Curves: SLPA results with (——) and without (- - - -) post-collisional effects. Experimental data: full symbols, proton impinging data by Cavalcanti *et al* [47] and DuBois *et al* [50]; open symbols, electron impinging data by Schram *et al* [52, 53].

for direct multiple ionization with the Poisson distribution (10). We also present total results including post-collisional contributions given by (18*a*) to (18*d*). To this end we employ recent yield spectra measurements of multicharged ions [20–31]. A summary of the yields employed for Ne, Ar, Kr and Xe is displayed in table 1.

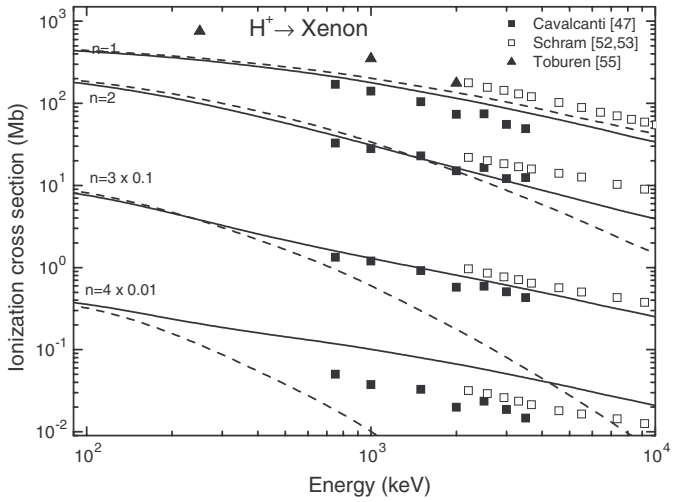

Figure 5. Single ($n = 1$), double ($n = 2$), triple ($n = 3$) and quadruple ($n = 4$) ionization cross sections of Xe by proton impact. Curves as in figure 4. Experimental data: full symbols, proton impinging data by Cavalcanti *et al* [47] and Toburen [55]; open symbols, electron impinging data by Schram *et al* [52, 53] .

Table 1. Experimental ratios $F_{\mathrm{nl},i}$, corresponding to post-collisional charge state distribution.

	Ne						Kr			
	1s				1s	2s	2p	3s	3p	3d
$F_{\mathrm{nl},1}$	1.5			$F_{\mathrm{nl},1}$	1	0.3	0	0	0	2
$F_{\mathrm{nl},2}$	93.5			$F_{\mathrm{nl},2}$	1.5	0.1	0.8	13	3.5	56
$F_{\mathrm{nl},3}$	4.8			$F_{\mathrm{nl},3}$	6	0.3	2.3	42	58.6	38
$F_{\mathrm{nl},4}$	0.3			$F_{\mathrm{nl},4}$	17	1	31	30	32.6	3
	(a)				(b)	(b)	(d)	(b)	(d)	(e)
	Ar						Xe			
	1s	2s	2p		3s	3p	3d	4p	4d	N shell
$F_{\mathrm{nl},1}$	0.7	0	0.5	$F_{\mathrm{nl},1}$	0	0	0	0	1	5
$F_{\mathrm{nl},2}$	10.5	1	86.2	$F_{\mathrm{nl},2}$	0	0	0.3	0	80	40
$F_{\mathrm{nl},3}$	7.8	89	13	$F_{\mathrm{nl},3}$	0	0	4	66	19	28
$F_{\mathrm{nl},4}$	42.7	10	0.3	$F_{\mathrm{nl},4}$	0	0	39	34	0	21
	(b)	(c)	(c)		(f)	(f)	(g)	(h)	(i)	(b)

(a) Morgan *et al* [21].
(b) Carlson *et al* [45].
(c) Brünken *et al* [23].
(d) Armen *et al* [22].
(e) Tamenori *et al* [24].
(f) Saito *et al* [26].
(g) Tamenori *et al* [27].
(h) Hayaishi *et al* [28].
(i) Kämmerling *et al* [29].

In general, the comparison of the SLPA cross sections with the experimental data is good at high impact energies, especially for the heaviest ions for which our many-electron model is expected to work better. The more electrons, the better our model works.

In figures 2 and 3, we compare the SLPA results for Ne and Ar, with those by Kirchner *et al* [6] obtained using the basis generator method (IPM). In both formalisms, the curves with and without including Auger-like contributions are displayed. The comparison of the curves without post-collisional corrections is interesting because it represents the comparison between quite different models (IPM and the SLPA). The inclusion of the Auger-like contributions is a second step and it is not supposed to introduce changes, except by the fact that the yields of post-collisional emission employed in [6] are different.

In both targets, Ne and Ar, the SLPA describes nicely the experimental values for single ionization, at least for proton energies above 500 keV. The inclusion of Auger emission in single ionization reduces the cross section (ionization of inner shells that ends in a higher ionization order). This difference is almost negligible for single ionization. Instead, for double, triple and quadruple ionization, the direct ionization curves fall down drastically with increasing impact energy, while the experimental result tends to show the same slope of the single ionization ones. As can be observed in these figures, the inclusion of Auger-like emission is mandatory in the high energy region. The comparison of figures 2 and 3 shows that the SLPA results are better for Ar than for Ne. In the latter, the direct multiple ionization curves (without Auger contribution) overestimate the data. The inclusion of post-collisional contributions corrects the slope at high energies.

Theoretical calculations on Kr and Xe may be heavy tasks for the IPM, depending on the number of subshells considered and on the treatment of the electronic dynamics. In contrast, the SLPA works better for multiple-electron targets, being more suitable to describe the d, or even the f shells, if any, than the s shells.

Results for multiple ionization of Kr and Xe, with and without post-collisional contributions, are displayed in figures 4 and 5. The total ionization curves including Auger contributions show a very good agreement even for triple ionization in both targets. For the quadruple ionization, the SLPA curves agree quite well with the data by DuBois [50] for Kr. In the case of Xe, the quadruple ionization curve has the same slope as the experimental data of Cavalcanti [47], with a factor of around 2 above.

The photoionization yields $F_{\mathrm{nl},i}$ $(i = 1, 4)$ employed in these calculations are those displayed in table 1. As can be observed in this table, the outer s shell of the rare gases is not included, i.e. there should not be Auger decay p–s in this case (see figure 4 in Brünken *et al* [23] for Ar^+ with a hole in the 3s shell).

For the Ne K shell, we use the $F_{1s,i}$ $(i = 1, 4)$ measured with time-of-flight (TOF) spectroscopy by Morgan *et al* [21]. For Ar L shell, we employed Brünken *et al* [23] data of $F_{2s,i}$ and $F_{2p,i}$ $(i = 1, 4)$ obtained by the photoelectron-ion coincidence technique. For the K shell no recent measurements were found in the literature, so we used the data by Carlson [45] using photoemission of the characteristic x-ray. The K shell contribution is important in quadruple-ionization of Ar.

In the case of Kr, the post-collisional contribution of each shell vacancy to i ionization $(i = 1, 4)$ is calculated by employing the experimental yields of TOF spectroscopy by Armen *et al* [22] ($F_{2p,i}$ and $F_{3p,i}$) and Tamemori *et al* [24] ($F_{3d,i}$), with the latter being the most important contribution to double and triple ionization of Kr at high energies. The 3s yield, $F_{3s,i}$, is that of Carlson [45]. The higher energy vacancies (1s, or 2s shells) produce cascade Auger processes that contribute mainly to Kr^{+q} production $(q > 4)$ [20]. Very recent measurement by Morishita *et al* [20] for distribution following ionization of 2p electrons of Kr introduce negligible differences in the final results.

For Xe, the post-collisional yields for the M shell are those measured by Tamenori *et al* [27] ($F_{3d,i}$ only, because 3p and 3s contribute to Xe^{+q} with $q > 4$ [26]). The main contribution to Xe double to quadruple ionization comes from ionization of the N shell. We found in the

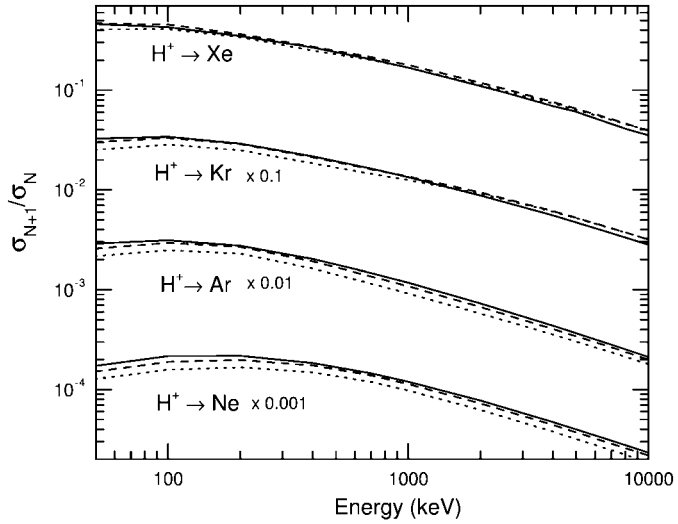

Figure 6. Ratios of SLPA ionization cross sections $\sigma_{(N+1)}/\sigma_N$ without post-collisional contributions, for protons in Ne, Ar, Kr and Xe. Curves: ——σ_2/σ_1; - - - -σ_3/σ_2; · · · · · ·σ_4/σ_3.

literature recent data by Hayaishi *et al* [28, 30] for the 4p shell, and by Karmmerling *et al* [29] for the 4d shell, but as far as we know, there are no measurements for Auger decay of the 4s shell. In this case, we employ the data by Carlson [45] which consider the N shell altogether. Future photoionization results for the decay of the 4s shell of Xe may introduce changes in the curves with post-collisional contribution in figure 5.

The difference between these new techniques and that of Carlson in 1966 [45] using characteristic x-rays is that even when the energy absorption is dominated by the shell whose energy is closest to that of the x-ray, photoabsorption can take place in any shell whose binding energy is less than the x-ray energy [45]. Carlson's data [45] (employed in recent multiple ionization calculations [6, 5, 8, 57]) cannot separate contributions due to ionization of outer shells.

Finally, we would like to call attention to the fact that the ratio $\sigma_{(N+1)}/\sigma_N$ without post-collisional contribution (only direct ionization of the electrons) follows the same tendency for $N = 1, 4$, as shown in figure 6. This sort of scaling can be very useful to estimate cross sections in high ionization processes.

4. Conclusions

We present a many-electron formalism to deal with a complex problem of atomic collisions, that is multiple ionization. This model is based on the transport equation method for an ion through an atom. This is our daring starting point, i.e. the Boltzman transport equation, usually employed along the extension of a foil, is concentrated inside the extension of a single atom.

Our model differs completely from the independent-particle approximation, leading us to the Poisson distribution for multiple scattering, instead of the multinomial distribution. Although it is well known that multinomial distribution tends to the Poisson one for a large number of electrons, conceptually they are quite different. Our probabilities take into account all the electrons of the shell, screening the penetrating ion. Moreover, our shell-to-shell

probabilities per atom may be larger than unity (meaning that more than one electron can be ionized), while the probabilities in the IPM must be rigorously smaller than unity. In addition, the mathematical requirements are simple, and the statistical representation of the electron cloud is better for multielectron systems, being equally simple to calculate He, Ne or Xe, for instance.

The inclusion of post-collisional contributions (time delay vacancy production following direct ionization of inner shells) is performed as a rearrangement of the Poisson distribution employing experimental ratios of charge state distribution of the target atoms measured with time-of-flight spectroscopy and photoelectron-ion coincidence techniques. Results are compared with experimental data for single-to-quadruple ionization of Ne, Ar, Kr and Xe by protons, showing very good accord.

Acknowledgments

This work was partially supported by the Consejo Nacional de Investigaciones Científicas y Técnicas, Argentina, the Agencia Nacional de Promoción Científica y Tecnológica and the Universidad de Buenos Aires.

References

[1] Gulyás L, Fainstein P D and Salin A 1995 *J. Phys. B: At. Mol. Opt. Phys.* **28** 245
[2] Stolterfoht N, DuBois R D and Rivarola R D 1997 *Electron Production Mechanism in Heavy Ion-atom Collisions* (Berlin: Springer)
[3] Kirchner T, Gulyás L, Lüdde H J, Henne A, Engel E and Dreizer R M 1997 *Phys. Rev. Lett.* **79** 1658
[4] Kirchner T, Horbasch M and Lüdde H J 2002 *Phys. Rev.* A **66** 052719
[5] Cavalcanti E G, Sigaud G M, Montenegro E C, Sant'Anna M M and Schmidt-Bocking H 2002 *J. Phys. B: At. Mol. Opt. Phys.* **35** 3937
[6] Spranger T and Kirchner T 2004 *J. Phys. B: At. Mol. Opt. Phys.* **37** 4159
[7] Jha L K, Kumar S and Roy B N 2006 *Eur. Phys. J.* D **40** 101
[8] Sigaud G M, Sant 'Ana M, Luna H, Santos A C F, McGrath C, Shah M B, Cavalcanti E G and Montenegro E C 2004 *Phys. Rev.* A **69** 062718
[9] Goudsmit S and Saunderson J L 1940 *Phys. Rev.* **57** 24
Goudsmit S and Saunderson J L 1940 *Phys. Rev.* **58** 36
[10] Sigmund P and Winterbon K B 1974 *Nucl. Instrum. Methods* **119** 541
[11] Scott W T 1963 *Rev. Mod. Phys.* **35** 231
[12] Remizovich V S, Tyazanov M I and Frolov V V 1985 *Sov. Phys. Dokl.* **30** 486
[13] Lencinas S and Burgdorfer J 1990 *Phys. Rev.* A **41** 1435
[14] Archubi C D and Arista N R 2005 *Phys. Rev.* A **72** 062712
[15] Archubi C D and Arista N R 2006 *Phys. Rev.* A **74** 052717
[16] Montanari C C, Miraglia J E and Arista N R 2003 *Phys. Rev.* A **67** 062702
[17] Montanari C C and Miraglia J E 2006 *Phys. Rev.* A **73** 024901
[18] Levine Z H and Louie S G 1982 *Phys. Rev.* B **25** 6310
[19] Lindhard J 1954 *K. Dan. Vidensk. Selsk. Mat.-Fys. Medd.* **28** 8
[20] Morishita Y, Tamenori Y, Okada K, Oyama T, Yamamoto K, Tabayashi K, Ibuki T, Moribayashi K and Suzuki I H 2006 *J. Phys. B: At. Mol. Opt. Phys.* **39** 1323
[21] Morgan D V, Sagurton M and Bartlett R J 1997 *Phys. Rev.* A **55** 1113
[22] Armen G B, Kanter E P, Krässig B, Levin J C, Southworth S H and Young L 2004 *Phys. Rev.* A **69** 062710
[23] Brünken S, Gerth Ch, Kanngieber B, Luhmann T, Richter M and Zimmermann P 2002 *Phys. Rev.* A **65** 042708
[24] Tamenori Y, Okada K, Tanimoto S, Ibuki T, Nagaoka S, Fujii A, Haga Y and Suzuki I H 2004 *J. Phys. B: At. Mol. Opt. Phys.* **37** 117
[25] Matsui T, Yoshii H, Tsukamoto K, Kawakita S, Murakami E, Adachi J, Yagishita A, Morioka Y and Hayaishi T 2004 *J. Phys. B: At. Mol. Opt. Phys.* **37** 3745
[26] Saito N and Suzuki I H 1992 *J. Phys. B: At. Mol. Opt. Phys.* **25** 1785
[27] Tamenori Y *et al* 2002 *J. Phys. B: At. Mol. Opt. Phys.* **35** 2799

[28] Hayaishi T, Matsui T, Yoshii H, Higurashi A, Murakami E, Yagishita A, Aoto T, Onuma T and Morioka Y 2002 *J. Phys. B: At. Mol. Opt. Phys.* **35** 141
[29] Karmmerling B, Krassig B and Schmidt V 1992 *J. Phys. B: At. Mol. Opt. Phys.* **25** 3621
[30] Hayaishi T, Yagishita T, Shigemasa E, Murakami E and Morioka Y 1990 *J. Phys. B: At. Mol. Opt. Phys.* **23** 4431
[31] Hikosaka Y, Aoto T, Lablaniquie P, Penent F, Shigemasa E and Ito K 2006 *J. Phys. B: At. Mol. Opt. Phys.* **39** 3457
[32] Ritchie R H 1959 *Phys. Rev.* **114** 644
[33] Echenique P M, Flores F and Ritchie R H 1990 *Solid. State Phys.* **43** 229
[34] Lindhard J and Winther A 1964 *K. Dan. Vidensk. Selsk. Mat.-Fys. Medd.* **34** 4
[35] Bonderup E 1967 *K. Dan. Vidensk. Selsk. Mat.-Fys. Medd.* **35** 17
[36] Rousseau C C, Chu W K and Powers D 1970 *Phys. Rev.* A **4** 1066
[37] Chu W K and Powers D 1972 *Rev. Lett.* A **40** 23
[38] Fuhr J D, Ponce V H, García de Abajo F J and Echenique P M 1998 *Phys. Rev.* B **57** 9329
[39] Montanari C C, Miraglia J E and Arista N R 2002 *Phys. Rev.* A **66** 042902
[40] Kadhane U, Montanari C C and Tribedi L C 2003 *Phys. Rev.* A **67** 032703
[41] Kadhane U, Montanari C C and Tribedi L C 2003 *J. Phys. B: At. Mol. Opt. Phys.* **36** 3043
[42] Kadhane U, Kumar A, Montanari C C and Tribedi L C 2006 *Rad. Phys. Chem* **75** 1542
[43] Bunge C F, Barrientos J A, Bunge A V and Cogordan J A 1992 *Phys. Rev.* A **46** 3691–3696
[44] Garcia A and Miraglia J E 2006 *Phys. Rev.* A **74** 059902
[45] Carlson T A, Hunt W E and Krause M O 1966 *Phys. Rev.* **151** 41
[46] DuBois R D and Manson S T 1987 *Phys. Rev.* A **35** 2007
[47] Cavalcanti E G, Sigaud G M, Montenegro E C and Schmidt-Bocking H 2003 *J. Phys. B: At. Mol. Opt. Phys.* **36** 3087
[48] Andersen L H, Hvelplund P, Knudsen H, Moller S P and Sorensen A H 1987 *Phys. Rev.* A **36** 3612
[49] Toburen L H, Manson S T and Kim Y-K 1978 *Phys. Rev.* A **17** 148
[50] DuBois R D, Toburen L H and Rudd M E 1984 *Phys. Rev.* A **29** 70
[51] Schram B L, Boerboom A J H and Kistermaker J 1966 *Physica* **32** 185
[52] Schram B L, de Heer F J, Van der Wiel M J and Kistermaker J 1965 *Physica* **31** 94
[53] Schram B L 1966 *Physica* **32** 197
[54] McCallion P, Shah M B and Gilbody H B 1992 *J. Phys. B: At. Mol. Opt. Phys.* **25** 1061
[55] Toburen L H 1974 *Phys. Rev.* A **9** 2505
[56] Müller A, Schuch B, Groh W and Salzborn E 1986 *Phys. Rev.* A **33** 3010
[57] Sant'Anna M M, Luna H, Santos A C F, McGrath C, Shah M B, Cavalcnti E G, Sigaud G M and Montenegro E C 2003 *Phys. Rev.* A **68** 042707